Circuit Design for Electrocardiography

Sagar Venkatesh Gubbi, Hiteshwar Rao, and Bharadwaj Amrutur, *Senior Member, IEEE*

Abstract

Electrocardiography (ECG or EKG) is the recording of electrical signals from the heart. This report discusses circuit design issues in building an electrocardiograph. A major impediment in acquiring ECG signals is the presence of 50 Hz power-line interference. In this report, a circuit model that captures the interference is presented. The circuit model is then used to analyze the performance characteristics of different interface circuits, and the superior performance of the so-called "driven right leg" based interface circuit is explained. An adaptive filter is found to be effective in digitally removing any remnant power line interference, although in most cases, this is not needed. Another issue in designing interface circuitry for ECG is the large impedance of the electrodes. This is mitigated by using an unconventionally biased amplifier with an even higher input impedance. Finally, this report observes that the low-impedance electrode in a 3-electrode system may be sized differently than the high impedance electrodes. This observation leads to a pseudo 2-electrode electrocardiograph which is actually a 3-electrode system with an inconspicuous third electrode.

I. Introduction

Electrocardiography (ECG) is a non-invasive way of recording the electrical activity of the heart. The cardiac tissue periodically generates a small electrical impulse that causes the heart to beat rhythmically. This electrical pulse reaches the surface of the skin with considerable attenuation, and it is this signal that has to be captured by the electrocardiograph (Fig. 1).

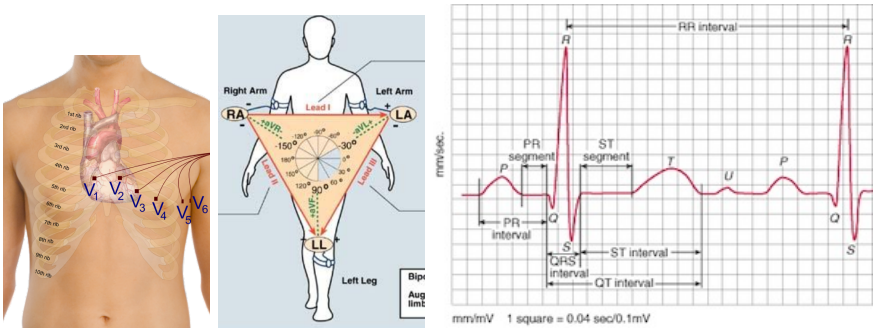

(a) Electrodes near the heart (b) Electrodes on the limbs (c) A sample electrocardiogram

Fig. 1. Sample electrode locations and a sample electrocardiogram.

The American Heart Association recommends that electrocardiographs should have a lower cut-off frequency not above 0.05 Hz and a higher cut-off frequency not below 100 Hz [1]. Furthermore, an amplitude error limit of 10 μV or 2% (whichever is higher) is recommended [1]. Typically, ECG signals have an amplitude of about 1 mV. But, depending on the location of the electrodes, it can be lower.

A major issue in acquiring ECG signals is the presence of power-line interference. Because the human body is good conductor of electricity compared to air, a small displacement current on the order of 100 nA flows through the body to the earth [2]. This manifests itself as a common mode voltage as seen by the electrocardiograph and can be substantially higher than the ECG signal itself. We shall model this phenomenon and analyze how well different circuit topologies keep this interference in check (Sections 2 and 3).

Good electrical contact between the skin and the electrode is assured by either abrading the skin and/or using a conductive gel. However, both of these methods cause significant inconvenience and are completely unsuitable for long-term ambulatory monitoring. To overcome this problem, dry-contact electrodes that require no skin preparation or conductive gels have been proposed [3]–[14]. But dry-contact electrodes have significantly larger impedance than wet-contact electrodes. Very high impedance amplifiers that make for suitable front-ends of dry-contact electrodes are discussed (Section 4).

The rest of this report is organized as follows. In Section 2, a circuit model that captures the effect of power-line interference is described. Subsequently, several interface circuit topologies are analyzed using this model (Section 3). Then, a very high impedance amplifier suited for dry-contact ECG front-ends is discussed (Section 4). Experimental results are presented in Section 5. Afterwords, a couple of pratical tips in building electrocardiographs are given (Section 6). Finally, some open issues are discussed in Section 7, and Section 8 concludes this report.

This report was written in May 2014. S.V.Gubbi, H.Rao, and B.Amrutur are with the Robert Bosch Center for Cyber-Physical Systems. e-mail: sagar.writeme@gmail.com, rao.hiteshwar@gmail.com, and amrutur@ece.iisc.ernet.in.

This work was funded by the Robert Bosch Centre for Cyber-Physical Systems, Indian Institute Of Science, Bangalore, India.

II. Circuit Model

Electrical power lines carrying high voltage at 50 Hz are ubiquitous. Because the human body is a good conductor of electricity compared to air, a small displacement current flows from the power lines through the human body to the ground. Along with the source of the ECG signal, this may be modeled by the circuit in Fig. 2. Values for the parasitic capacitances are from [2].

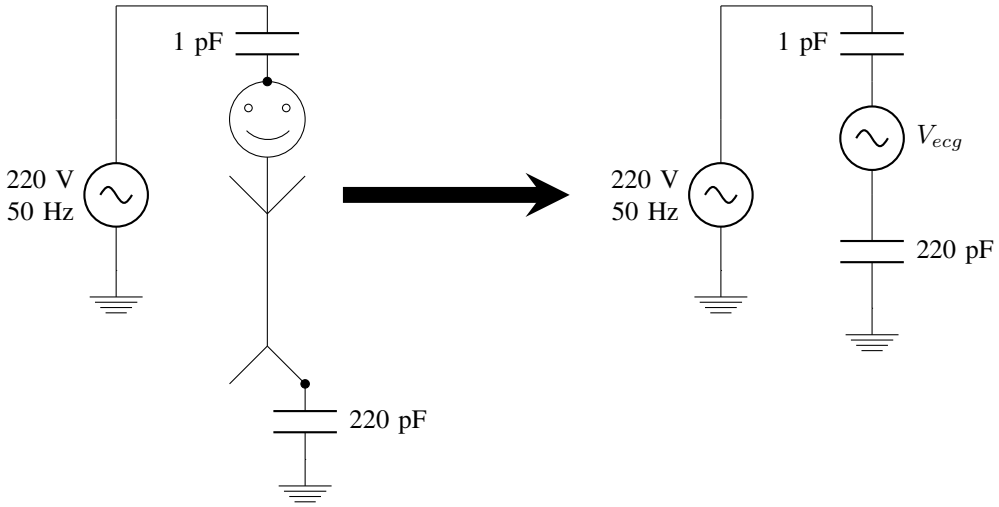

Fig. 2. Electrical model of the human body.

III. Performance of interface circuit configurations

The performance of different interface circuit configurations is analyzed using the electrical model developed in the previous section. Z_e is the electrode-skin impedance (if there are two sensing electrodes, the impedances are Z_{e1} and Z_{e2}), Z_i is the input impedance of a unity gain buffer, Z_g is the electrode-skin impedance of the low-impedance electrode, and Z_s is the isolation impedance between the circuit command and the earth ground. All node voltages with a single subscript are with respect to earth ground and *not* circuit common (Example: V_g). Z_i of hi-z buffers is in the order of 1 GΩ. For copper dry-contact electrodes of 1 cm^2 size, Z_e is typically around 1 MΩ [15]. In battery operated circuits that are isolated from the earth ground, Z_s is around 3 pF (1 GΩ at 50 Hz) [2].

A. Two-electrode Single Ended Interface Circuit

In this configuration (Fig. 3), one of the electrodes is connected to a high impedance unity gain amplifier (described in Section 4). The second electrode is a low impedance electrode that is connected to the circuit common (V_g).

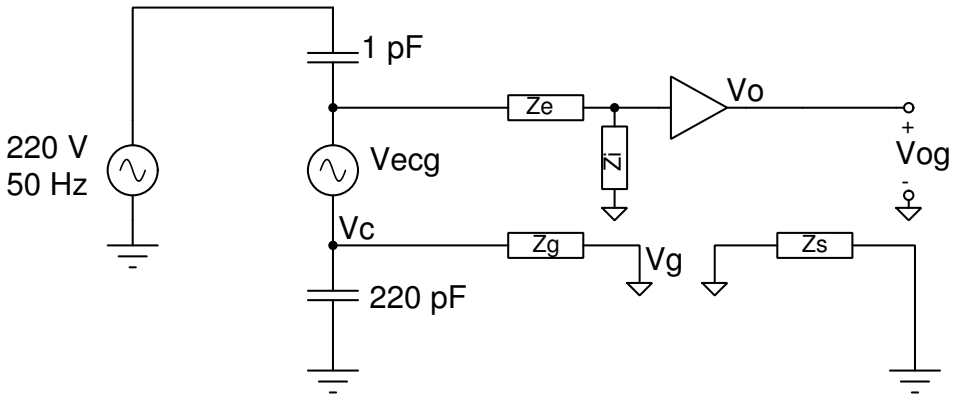

Fig. 3. Two-electrode single ended interface circuit

Since the isolation impedance between the ECG interface circuit and the earth ground is substantially larger than the human body to earth ground impedance,

$$V_c \approx \frac{\frac{1}{220p}}{\frac{1}{1p}+\frac{1}{220p}} \times 220V, 50Hz \approx 1V, 50Hz \tag{1}$$

Some of the displacement current due to the 220 V power line flows from the body to the earth ground via the interface circuit.

$$\frac{V_c - V_g}{Z_g} = \frac{V_g}{Z_s} \tag{2}$$

Thus,

$$V_g = \frac{Z_s}{Z_s + Z_g} V_c \tag{3}$$

Equation (3) shows that as isolation impedance between the circuit common and the earth ground increases, the circuit common comes closer to the potential of the body and thus less of the 50 Hz common mode power line interference is seen.

Finally,

$$V_{og} = V_o - V_g = \frac{Z_i}{Z_e + Z_i}(V_c + V_{ecg} - V_g) = \frac{Z_i}{Z_e + Z_i}\left(\frac{Z_g}{Z_s + Z_g} V_c + V_{ecg}\right) \tag{4}$$

Simplifying,

$$V_{og} = \left(\frac{Z_i}{Z_e + Z_i} \cdot \frac{Z_g}{Z_s + Z_g}\right) V_c + \left(\frac{Z_i}{Z_e + Z_i}\right) V_{ecg} \tag{5}$$

Even if the two electrode impedances are matched (i.e.. $Z_g = Z_e$), the output seen by the circuit contains substantial power-line interference. Thus, this circuit is not recommended. A sample implementation of the 2-electrode single ended interface circuit may be found in [16].

B. Two-electrode Differential Interface Circuit

In this configuration (Fig. 4), both the electrodes are connected to high impedance unity gain amplifiers. The circuit common is left floating and is connected to earth ground only via a large isolation impedance (Z_s).

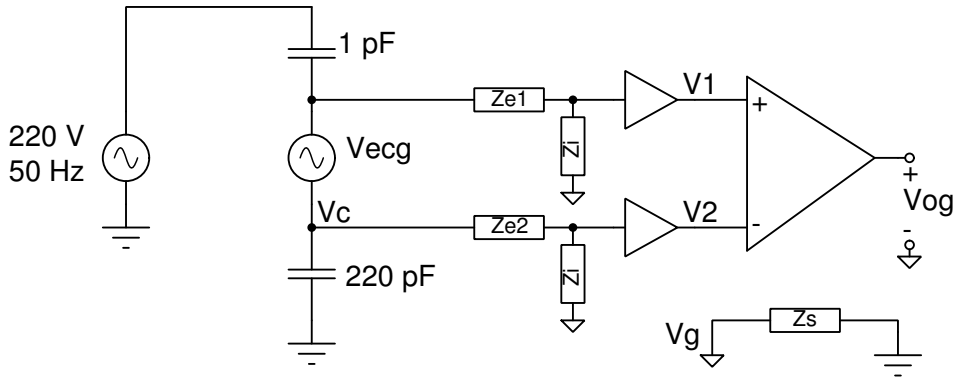

Fig. 4. Two-electrode differential interface circuit

The isolation impedance drags the circuit common weakly towards earth ground.

$$V_g = 0 \tag{6}$$

After the unity gain buffers,

$$V_2 = \frac{Z_i}{Z_{e2} + Z_i} V_c \tag{7}$$

$$V_1 = \frac{Z_i}{Z_{e1} + Z_i}(V_c + V_{ecg}) \tag{8}$$

Thus, for small electrode imbalances ($Z_{e1} \approx Z_{e2}$),

$$V_{og} = V_1 - V_2 = \frac{\frac{\Delta Z_e}{Z_i}}{\left(1 + \frac{Z_e}{Z_i}\right)^2} V_c + \frac{Z_i}{Z_i + Z_{e1}} V_{ecg} \tag{9}$$

where $\Delta Z_e = Z_{e2} - Z_{e1}$ and $Z_e = \frac{Z_{e1} + Z_{e2}}{2}$. Although in this configuration, when the electrode impedances are matched the interference vanishes, it is inadvisable to use this because (a) The circuit common is floating, and (b) High common mode impedance is unforgiving to static voltages that develop on the body, and this can cause the amplifiers to saturate [2]. These problems can be surmounted by having a topology with low common mode input impedance and high differential mode impedance [17]–[19]. However, this is not recommended because differential input impedance is limited by component tolerances. It turns out that both high common mode impedance and low common mode impedance result in low power-line interference [20], but low common mode impedance is more suitable since it is resistant to static charges on the body. The right leg drive based three-electrode interface discussed in a subsequent section has simpler circuitry and offers better performance.

C. Three-electrode Interface circuit with passive ground

In this configuration (Fig. 14), the two sensing electrodes are connected to high impedance unity gain amplifiers. The third low-impedance electrode is connected to the circuit common.

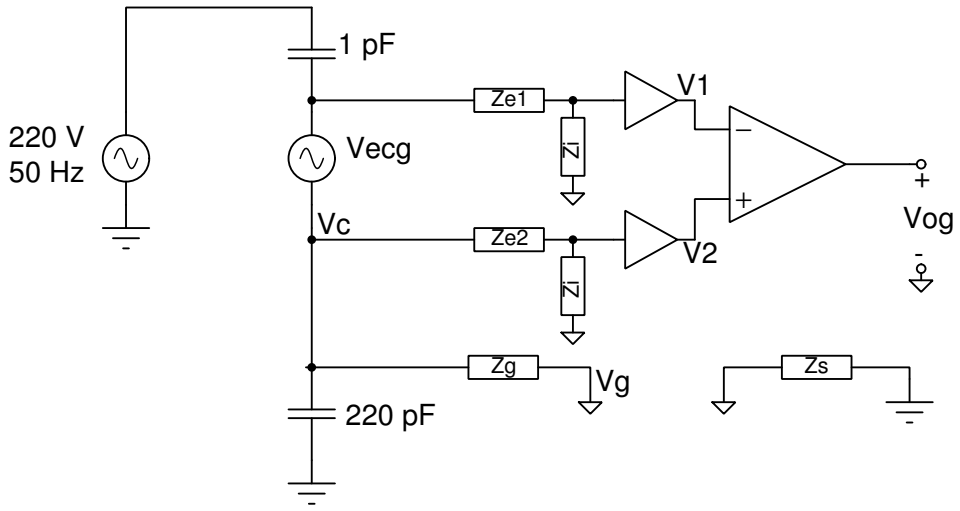

Fig. 5. Three-electrode interface circuit with passive dry ground

Similar to subsection A,

$$V_g = \frac{Z_s}{Z_s + Z_g} V_c \tag{10}$$

And,

$$V_1 = Vg + \frac{Z_i}{Z_i + Z_{e1}} \left(V_c + V_{ecg} - V_g \right) \tag{11}$$

$$V_2 = Vg + \frac{Z_i}{Z_i + Z_{e2}} \left(V_c - V_g \right) \tag{12}$$

Thus,

$$V_{og} = \left(\frac{Z_i}{Z_i + Z_{e1}} - \frac{Z_i}{Z_i + Z_{e2}} \right) \frac{Z_g}{Z_s + Z_g} V_c + \frac{Z_i}{Z_i + Z_{e1}} V_{ecg} \tag{13}$$

For small electrode mismatches ($Z_{e1} \approx Z_{e2}$),

$$V_{og} = \left(\frac{\frac{\Delta Z_e}{Z_i}}{\left(1 + \frac{Z_e}{Z_i} \right)^2} \cdot \frac{Z_g}{Z_s + Z_g} \right) V_c + \frac{Z_i}{Z_i + Z_{e1}} V_{ecg} \tag{14}$$

where $\Delta Z_e = Z_{e2} - Z_{e1}$ and $Z_e = \frac{Z_{e1} + Z_{e2}}{2}$. When the two electrodes are matched, the power-line interference vanishes. Furthermore, when the isolation impedance (Z_s) is large as in the case of battery powered systems, the low-impedance connection to the body (Z_g) suppresses the interference when there is an electrode mismatch. While this configuration can be used, the driven right leg circuit described in the next subsection is even more effective at suppressing power line interference in the presence of electrode mismatches, and thus it should be preferred.

D. Three-electrode Interface circuit with driven right leg

In this configuration (Fig. 6), the two sensing electrodes are connected to high impedance unity gain amplifiers. The third low-impedance electrode is driven an amplified and inverted version of the common mode signal.

To simplify calculations, we shall initially assume that $Z_i = \infty$. Then,

$$V_2 = V_c \tag{15}$$

and

$$V_1 = V_c + V_{ecg} \tag{16}$$

The right leg drive amplifier amplifiers the common mode voltage to give

$$V_{RLD} = -A \left(\frac{V_1 + V_2}{2} \right) + V_g \tag{17}$$

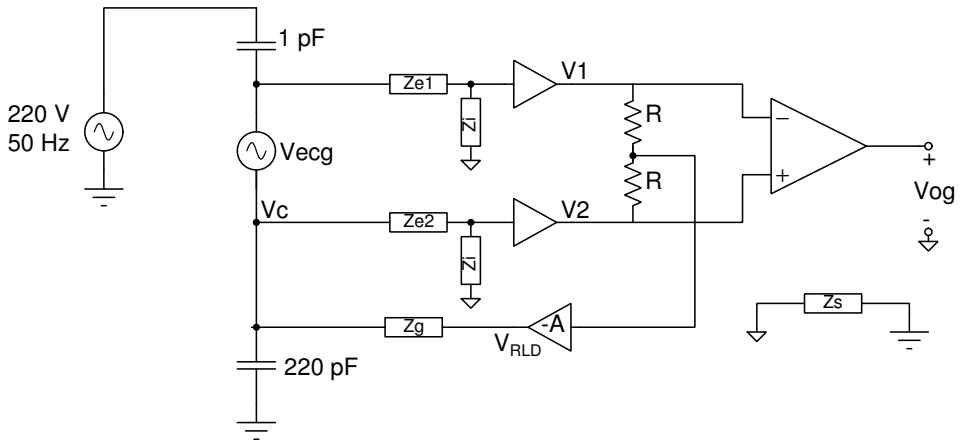

Fig. 6. Three-electrode interface circuit with driven ground

$$V_{RLD} = -A\left(V_c - V_g + \frac{V_{ecg}}{2}\right) + V_g \tag{18}$$

Now, we can calculate the circuit common potential V_g.

$$\frac{V_c - V_{RLD}}{Z_g} = \frac{V_g}{Z_s} \tag{19}$$

Assuming that $A >> 1$,

$$\frac{V_c}{Z'_g} + \frac{V_{ecg}}{2Z'_g} = \frac{V_g}{Z_s} + \frac{V_g}{Z'_g} \tag{20}$$

where $Z'_g = \frac{Z_g}{A+1}$. Thus,

$$V_g = \frac{Z_s}{Z_s + Z'_g}V_c + \frac{Z_s}{Z_s + Z'_g}\frac{V_{ecg}}{2} \tag{21}$$

Let us now return to the case when $Z_i < \infty$ and calculate the output voltage.

$$V_{1g} = V_1 - V_g = (V_c + V_{ecg} - V_g)\frac{Z_i}{Z_i + Z_{e1}} \approx \left(\frac{Z'_g}{Z_s}V_c + \frac{V_{ecg}}{2}\right)\frac{Z_i}{Z_i + Z_{e1}} \tag{22}$$

$$V_{2g} = V_1 - V_g = (V_c - V_g)\frac{Z_i}{Z_i + Z_{e1}} \approx \left(\frac{Z'_g}{Z_s}V_c - \frac{V_{ecg}}{2}\right)\frac{Z_i}{Z_i + Z_{e2}} \tag{23}$$

If the electrode imbalance is small,

$$V_{og} = V_{1g} - V_{2g} = \left(\frac{Z'_g}{Z_s}\frac{\frac{\Delta Z_e}{Z_i}}{\left(1 + \frac{Z_e}{Z_i}\right)^2}\right)V_c + \left(\frac{Z_i}{Z_i + Z_e}\right)V_{ecg} \tag{24}$$

where $\Delta Z_e = Z_{e2} - Z_{e1}$ and $Z_e = \frac{Z_{e1}+Z_{e2}}{2}$. This is similar to Eq. (14) with Z_g replaced by Z'_g. Thus, with right leg drive, the electrode-skin impedance of the low-impedance electrode effectively gets divided by the right leg drive gain (A). A more detailed discussion of common mode interference and the right leg drive circuit may be found at [21], [22] and [23].

Table I compares the performance of the four interface circuit configurations discussed. The general trend is that power-line interference reduces as the electrode imbalance decreases and the influence of electrode imbalance becomes smaller as the input impedance of the front-end amplifier increases.

Let us consider some typical numerical values for battery powered copper dry-contact electrodes of size 1 cm^2. Suppose $Z_i = 100\ M\Omega$, $Z_e = Z_g = 10\ M\Omega$, $\Delta Z_e = 500\ k\Omega$, $Z_s = 1\ G\Omega$, $V_c \approx 1V, 50Hz$, and for the right leg drive $A = 100$. The

TABLE I
NOISE ESTIMATION PERFORMANCE

Circuit configuration	V_{og}	Typical values
2-electrode, single ended	$V_{og} = \left(\frac{Z_i}{Z_e+Z_i} \cdot \frac{Z_g}{Z_s+Z_g}\right) V_c + \left(\frac{Z_i}{Z_e+Z_i}\right) V_{ecg}$	$V_{og} = 10\ mV_{50Hz} + 1\ mV_{ecg}$
2-electrode, differential	$V_{og} = \left(\frac{\frac{\Delta Z_e}{Z_i}}{\left(1+\frac{Z_e}{Z_i}\right)^2}\right) V_c + \left(\frac{Z_i}{Z_i+Z_{e1}}\right) V_{ecg}$	$V_{og} = 5\ mV_{50Hz} + 1\ mV_{ecg}$
3-electrode, passive ground	$V_{og} = \left(\frac{\frac{\Delta Z_e}{Z_i}}{\left(1+\frac{Z_e}{Z_i}\right)^2} \cdot \frac{Z_g}{Z_s+Z_g}\right) V_c + \left(\frac{Z_i}{Z_i+Z_{e1}}\right) V_{ecg}$	$V_{og} = 50\ \mu V_{50Hz} + 1\ mV_{ecg}$
3-electrode, driven-right-leg	$V_{og} = \left(\frac{\frac{\Delta Z_e}{Z_i}}{\left(1+\frac{Z_e}{Z_i}\right)^2} \cdot \frac{Z'_g}{Z_s+Z'_g}\right) V_c + \left(\frac{Z_i}{Z_i+Z_e}\right) V_{ecg}$	$V_{og} = 0.5\ \mu V_{50Hz} + 1\ mV_{ecg}$

third column in Table I gives a feel for the performance of different interface circuit configurations using these parameters. The first term in the third column represents the amplitude of the power-line interference and the second term represents the amplitude of the ECG signal (assumed to be 1 mV). The right leg drive configuration results in the least power-line interference.

Several methods have been proposed to remove the remnant power-line interference due to electrode imbalance. Sophisticated phase sensitive detection has been used in [24] to tilt the gain in the differential amplifier and favor one of the electrodes so as to neutralize the electrode imbalance. A Phase Locked Loop (PLL) and a lock-in amplifier (LIA) have been used in [25] to lock on to the interference signal and cancel it. An adaptive filter in the digital domain can also be used to cancel power-line interference [26]–[29]. Among these techniques, the adaptive filter in [29] is preferable because it is robust and needs no additional hardware.

Finally, ultra-low power discrete and integrated implementations of variants of these circuits are described in [30] and [31] respectively.

IV. INPUT IMPEDANCE

The input impedance of the front-end amplifier forms a potential divider with the electrode impedance. Furthermore, as seen in the previous section, a smaller input impedance exacerbates the effect of electrode imbalance resulting in larger power-line interference. Thus, it is desirable to have large input impedance in the front-end amplifiers. This is achieved in the so-called "active electrodes" by placing the amplifier right on top of the electrode, thereby reducing the loss of input impedance in the cable that attaches the electrode to the circuitry [32]. Degen et al. go one step further and amplify the ECG signal on the electrode itself at the cost of larger interference due to gain mismatch [33].

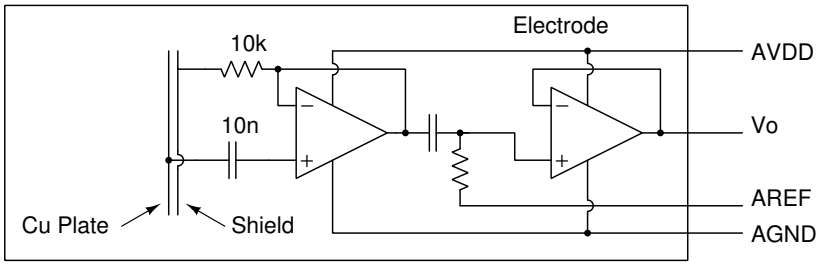

Fig. 7. Schematic of the electrode. The sensing copper plate is the backside of the PCB. The components are assembled on the front side. The copper plate will be in contact with the skin, and the driven shield in the inner plane of the PCB serves to reduce input capacitance.

The use of bootstrapped amplifiers has been proposed in [2], [34] to achieve large input impedance in the front-end amplifier. However, bootstrapping worsens noise performance. In [32] and more recently in [11], [15], rail-to-rail input/output (RRIO) opamps have been used with the positive terminal left floating (Fig. 7). This is based on the idea that a small leakage current through the input protection diodes on the hi-z positive terminal will bias the op-amp. It is possible, even likely, that the bias point will be close to one of the rails because of mismatch in the input protection diodes and other parasitics. However, the ECG amplitude being only a few mV at most will have no trouble passing through the RRIO unity gain amplifier. This signal is subsequently high-pass filtered so as to not overwhelm the subsequent stages with a signal close to the rails.

V. EXPERIMENTAL RESULTS

Figure 8 shows the schematic of the prototype electrocardiograph[1]. A 12-bit ADC was used with a sample rate of 400 Hz. Although Fig. 8 depicts the inner plane of the PCB being used as a shield, our implementation was on a 2-layer PCB with no such shield.

[1]The complete schematic and software are available under an open source license at https://github.com/s-gv/ecg

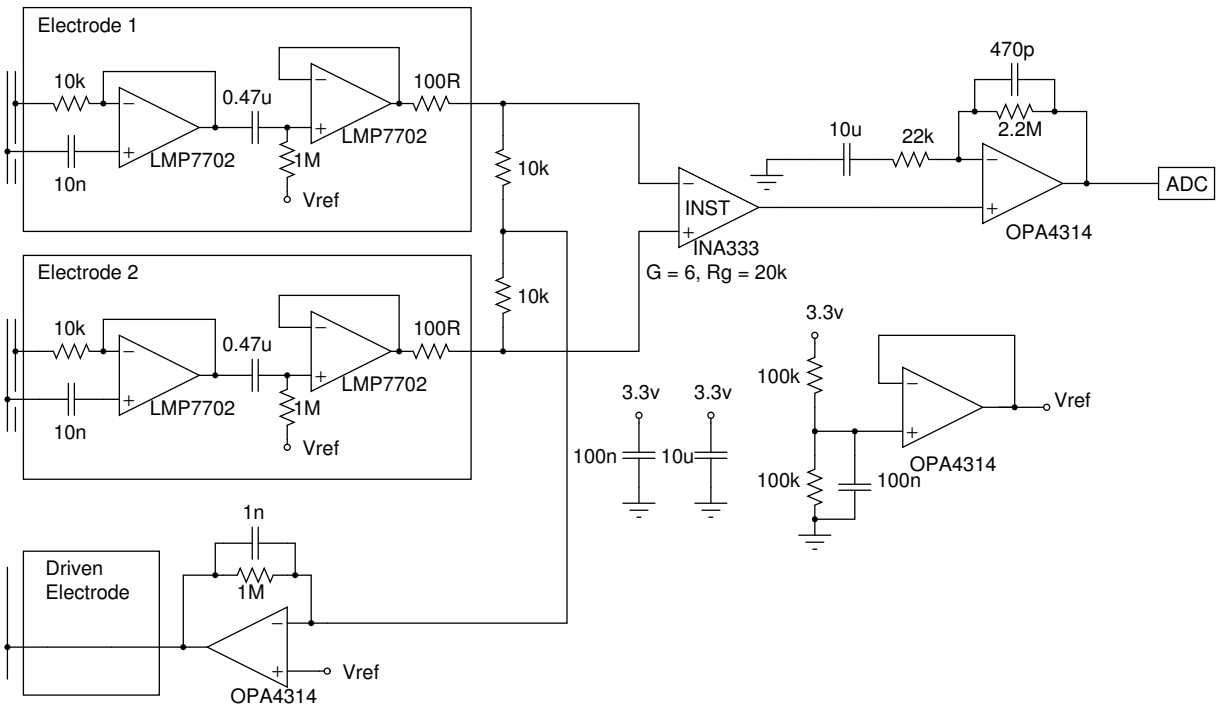

Fig. 8. Schematic of the prototype electrocardiograph. 20k instead of 22k in the final stage. 680p instead of 1n in the RLD stage.

As discussed previously, in the driven right leg configuration, the electrode impedance of the low-impedance driven electrode is effectively divided by the gain of the feedback amplifier. Thus, the low-impedance electrode may be sized considerably smaller than the high impedance sensing electrodes. We christen this "pseudo 2-electrode" ECG, wherein the outer ring of one of the electrodes is connected to the output of the right leg drive amplifier (Fig. 9).

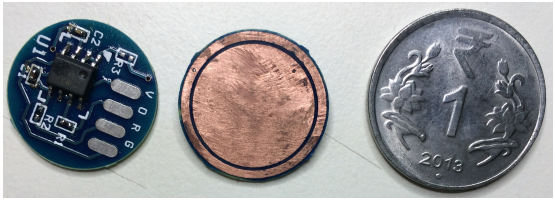

(a) Electrodes (Diameter $\approx$ 18 mm)

Fig. 9. Photo of the wearable electrocardiograph.

Figure 10 shows a sample electrocardiogram recorded using the "pseudo 2-electrode" configuration. The two electrodes (in one of which the outer ring was the driven electrode) were pressed across the heart. Power-line interference is not noticeable.

Figure 11 shows a sample electrocardiogram recorded in a Faraday cage using the single ended 2-electrode configuration. The raw signal shows significant power-line interference, and it is quite difficult to make out any features in the electrocardiogram. After adaptive filtering [29], the QRS spike is observable.

VI. Practical tips

Based on our experience in designing an electrocardiograph, we offer the following gotchas.

- ***Waveforms in the oscilloscope are better than they appear***. In some bench-top oscilloscopes, one of the terminals of the probe is connected to earth ground. So, connecting such a probe to the ECG interface circuit effectively makes $Z_s = 0$. Even otherwise, bench-top oscilloscopes are usually mains powered, which substantially decreases the isolation impedance (from 0.1-1 pF to 10 pF). Consequently, if you are observing voltages on a battery powered ECG interface circuit using a line-powered oscilloscope, expect to see 10-100x more power-line interference than if you don't connect the oscilloscope.
- ***Battery charger corrupts ECG signals***. When prototyping electrocardiographs, be vary of the power source. It's not that you need a very clean power source devoid of 50 Hz interference. The real problem is how much isolation impedance there is between the power source and the earth ground. If you're designing battery powered equipment, do *not* use mains powered bench-top power supplies or draw power from a USB cable attached to a mains powered PC when prototyping.

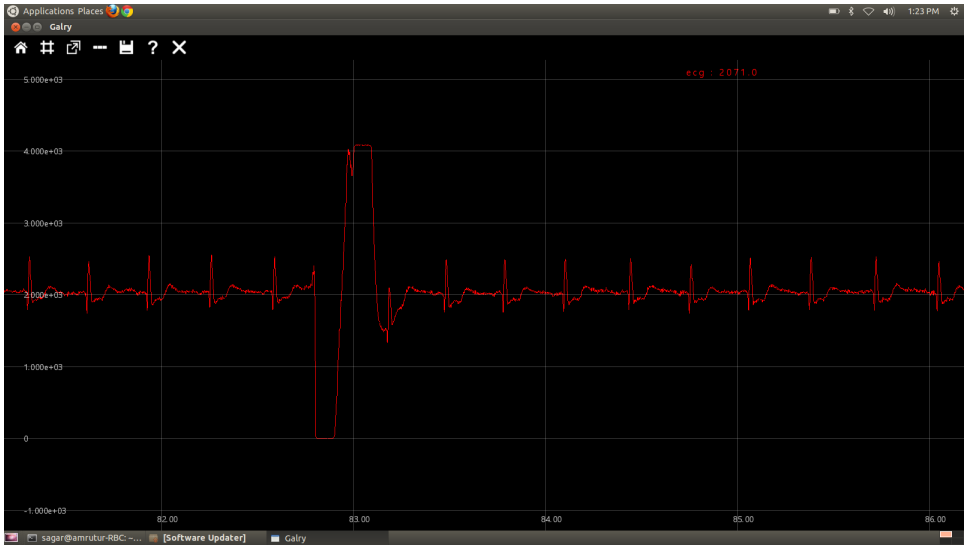

Fig. 10. A sample electrocardiogram recorded using "pseudo 2-electrodes"

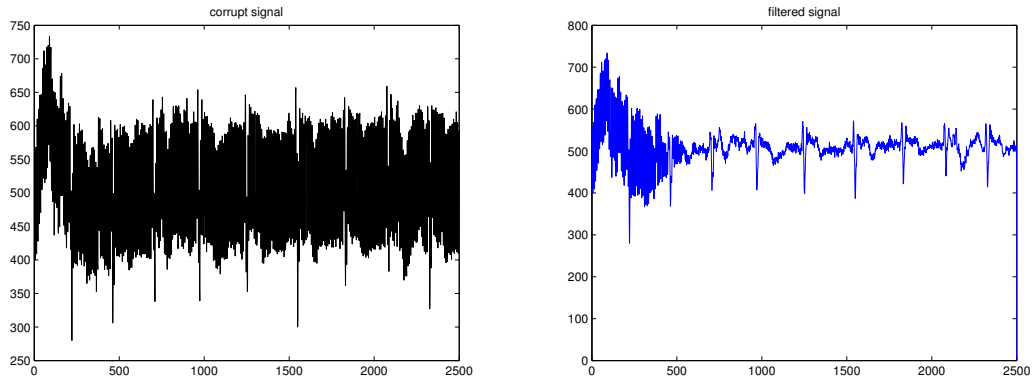

(a) Raw electrocardiogram

(b) Filtered electrocardiogram

Fig. 11. A sample electrocardiogram recorded using two electrodes in the single ended mode

The power-line interference will be 10-100x higher than if you used a battery powered circuit because of the lowered isolation impedance. It is acceptable to draw power from the USB port of a laptop when prototyping. But do not forget to remove the battery charger from the laptop ! Also, if you're using a laptop as the power source, keep the laptop and the interface circuit PCB on your lap rather than on a table nearby.

- ***Large power-line noise despite using a 50 Hz notch filter***. Notch filters are unforgiving to frequency deviations. If you have a steep notch filter that rejects 50 Hz interference, it'll do a fairly bad job if the power line frequency is 49 Hz and not 50 Hz. The situation can be worse if an analog notch filter is used (because of component tolerances). Furthermore, notch filters tend to cause ringing artifacts near the QRS spike. An adaptive filter [29] is immune to these problems and should thus be preferred[2].
- ***Underestimating the electrode-skin impedance***. The electrode-skin impedance for dry/non contact electrodes is quite high. So, the amplifier has to be placed very close to the skin to ensure that input impedance is large. Otherwise, the parasitic impedance of the wire will form a potential divider with the electrode impedance and cause substantial attenuation of the ECG signal (Fig. 12).

VII. Open Issues

Dry-contact electrodes were demonstrated decades ago [3]. Despite the convenience they offer, dry-contact electrodes have not seen widespread deployment. One of the reasons is that they are much more susceptible to motion artifacts than gel-based wet electrodes. In wet electrodes, the gel, in addition to lowering the electrode impedance, also serves as an adhesive and

[2]An open source implementation of the adaptive filter in [29] is available at https://github.com/s-gv/ecg/blob/master/adaptive_filter/pll_martens_errorfilt_supp.m

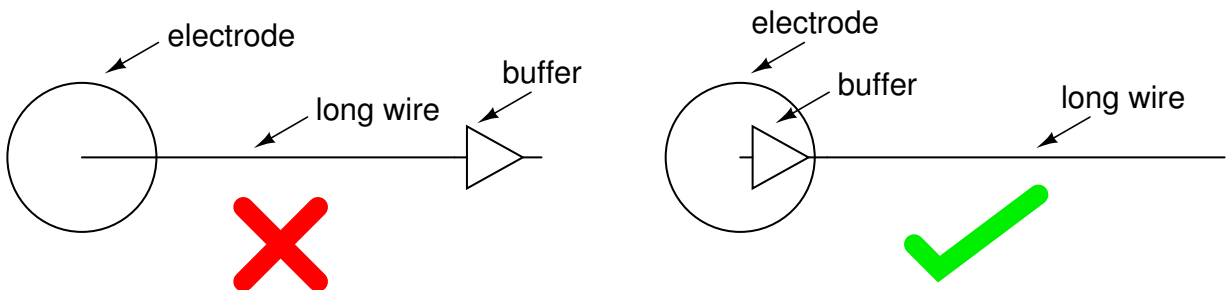

Fig. 12. How to not build an electrode with a long cable

reduces the relative motion between the skin and the electrode, thereby reducing motion artifacts. In dry electrodes, however, there is nothing to prevent relative motion between the electrodes and the skin. The prevailing opinion is that a mechanical (product design) solution is needed to solve this problem [15]. It remains open if the problem of motion artifacts can be solved by clever artifact cancelling algorithms.

Another open issue with dry-contact electrodes is the size of the electrodes. To the best of our knowledge, no systematic study that recommends a particular size for the high-impedance and low-impedance electrodes has been done, and there has been no discussion on whether PCB layout or product design strategies can help reduce the electrode size.

Currently, even in wireless ECG systems, the electrodes need to be connected by wires. At the time of writing, no truly wireless ECG system exists. In such a system, the electrodes will have a wireless module and can work without any wires. The question of how build such a fully wireless electrocardiograph (with wireless electrodes) remains open.

Finally, existing electrocardiograph designs in the literature do not attempt minimize the number of off-chip components when using a popular commercially available SoCs that include a radio and a microcontroller (example: TI's CC2540). It is desirable to reduce the number of analog components required to build an electrocardiograph because it will help in making a compact product without resorting to expensive custom integrated circuits. Multiple amplifiers are currently needed to build an electrocardiograph. It would be worthwhile exploring if an electrocardiograph can be built with few off-chip components by exploiting peripherals available in a microcontroller platform.

VIII. Conclusion

An electrical model of the human body was presented. This model explained the superior performance of the right-leg-driven interface circuit from the perspective of power-line interference. An adaptive filter was found to be most suitable in removing any remnant power-line interference due to electrode imbalance. A number of practical suggestions to aid prototyping battery powered ECG systems were given, and some open issues were discussed.

Acknowledgment

The authors would like to thank Pushkar and Manikandan for fruitful discussions. We also thank Dhruv Saxena for product design assistance.

References

[1] J. J. Bailey, A. S. Berson, A. Garson Jr, L. G. Horan, P. W. Macfarlane, D. W. Mortara, and C. Zywietz, "Recommendations for standardization and specifications in automated electrocardiography: bandwidth and digital signal processing. a report for health professionals by an ad-hoc writing group of the committee on electrocardiography and cardiac electrophysiology of the council on clinical cardiology, american heart association." *Circulation*, vol. 81, no. 2, p. 730, 1990.

[2] N. V. Thakor and J. G. Webster, "Ground-free ECG recording with two electrodes," *IEEE Transactions on Biomedical Engineering*, no. 12, pp. 699–704, 1980.

[3] A. Lopez and P. C. Richardson, "Capacitive electrocardiographic and bioelectric electrodes," *IEEE Transactions on Biomedical Engineering*, no. 1, pp. 99–99, 1969.

[4] C. R. Merritt, H. T. Nagle, and E. Grant, "Fabric-based active electrode design and fabrication for health monitoring clothing," *IEEE Transactions on Information Technology in Biomedicine*, vol. 13, no. 2, pp. 274–280, 2009.

[5] M. Steffen, A. Aleksandrowicz, and S. Leonhardt, "Mobile noncontact monitoring of heart and lung activity," *IEEE Transactions on Biomedical Circuits and Systems*, vol. 1, no. 4, pp. 250–257, 2007.

[6] J. Yoo, L. Yan, S. Lee, H. Kim, and H.-J. Yoo, "A wearable ECG acquisition system with compact planar-fashionable circuit board-based shirt," *IEEE Transactions on Information Technology in Biomedicine*, vol. 13, no. 6, pp. 897–902, 2009.

[7] T.-H. Kang, C. R. Merritt, E. Grant, B. Pourdeyhimi, and H. T. Nagle, "Nonwoven fabric active electrodes for biopotential measurement during normal daily activity," *IEEE Transactions on Biomedical Engineering*, vol. 55, no. 1, pp. 188–195, 2008.

[8] M. Ishijima, "Monitoring of electrocardiograms in bed without utilizing body surface electrodes," *IEEE Transactions on Biomedical Engineering*, vol. 40, no. 6, pp. 593–594, 1993.

[9] T. J. Sullivan, S. R. Deiss, and G. Cauwenberghs, "A low-noise, non-contact EEG/ECG sensor," in *IEEE Biomedical Circuits and Systems Conference*, 2007, pp. 154–157.

[10] Y. M. Chi, S. R. Deiss, and G. Cauwenberghs, "Non-contact low power EEG/ECG electrode for high density wearable biopotential sensor networks," in *IEEE Sixth International Workshop on Wearable and Implantable Body Sensor Networks*, 2009, pp. 246–250.

[11] Y. M. Chi, P. Ng, E. Kang, J. Kang, J. Fang, and G. Cauwenberghs, "Wireless non-contact cardiac and neural monitoring," in *Wireless Health*. ACM, 2010, pp. 15–23.
[12] Y. M. Chi and G. Cauwenberghs, "Wireless non-contact EEG/ECG electrodes for body sensor networks," in *IEEE International Conference on Body Sensor Networks (BSN)*, 2010, pp. 297–301.
[13] ——, "Micropower non-contact eeg electrode with active common-mode noise suppression and input capacitance cancellation," in *Annual International Conference of the IEEE Engineering in Medicine and Biology Society*, 2009, pp. 4218–4221.
[14] T. J. Sullivan, S. R. Deiss, T.-P. Jung, and G. Cauwenberghs, "A brain-machine interface using dry-contact, low-noise EEG sensors," in *IEEE International Symposium on Circuits and Systems*, 2008, pp. 1986–1989.
[15] Y. Chi, T.-P. Jung, and G. Cauwenberghs, "Dry-contact and noncontact biopotential electrodes: Methodological review," *IEEE Reviews in Biomedical Engineering*, vol. 3, pp. 106–119, 2010.
[16] W. P. Holsinger and K. M. Kempner, "Portable ekg telephone transmitter," *IEEE Transactions on Biomedical Engineering*, no. 4, pp. 321–323, 1972.
[17] D. Dobrev and I. Daskalov, "Two-electrode biopotential amplifier with current-driven inputs," *Medical and Biological Engineering and Computing*, vol. 40, no. 1, pp. 122–127, 2002.
[18] D. Dobrev, "Two-electrode low supply voltage electrocardiogram signal amplifier," *Medical and Biological Engineering and Computing*, vol. 42, no. 2, pp. 272–276, 2004.
[19] D. P. Dobrev, T. Neycheva, and N. Mudrov, "Bootstrapped two-electrode biosignal amplifier," *Medical & biological engineering & computing*, vol. 46, no. 6, pp. 613–619, 2008.
[20] E. M. Spinelli and M. A. Mayosky, "Two-electrode biopotential measurements: power line interference analysis," *IEEE Transactions on Biomedical Engineering*, vol. 52, no. 8, pp. 1436–1442, 2005.
[21] B. B. Winter and J. G. Webster, "Reductionl of interference due to common mode voltage in biopotential amplifiers," *IEEE Transactions on Biomedical Engineering*, no. 1, pp. 58–62, 1983.
[22] J. C. Huhta and J. G. Webster, "60-hz interference in electrocardiography," *IEEE Transactions on Biomedical Engineering*, no. 2, pp. 91–101, 1973.
[23] B. B. Winter and J. G. Webster, "Driven-right-leg circuit design," *IEEE Transactions on Biomedical Engineering*, no. 1, pp. 62–66, 1983.
[24] T. Degen and H. Jackel, "Enhancing interference rejection of preamplified electrodes by automated gain adaption," *IEEE Transactions on Biomedical Engineering*, vol. 51, no. 11, pp. 2031–2039, 2004.
[25] I.-D. Hwang and J. G. Webster, "Direct interference canceling for two-electrode biopotential amplifier," *IEEE Transactions on Biomedical Engineering*, vol. 55, no. 11, pp. 2620–2627, 2008.
[26] B. Widrow, J. R. Glover Jr, J. M. McCool, J. Kaunitz, C. S. Williams, R. H. Hearn, J. R. Zeidler, E. Dong Jr, and R. C. Goodlin, "Adaptive noise cancelling: Principles and applications," *Proceedings of the IEEE*, vol. 63, no. 12, pp. 1692–1716, 1975.
[27] N. V. Thakor and Y.-S. Zhu, "Applications of adaptive filtering to ecg analysis: noise cancellation and arrhythmia detection," *IEEE Transactions on Biomedical Engineering*, vol. 38, no. 8, pp. 785–794, 1991.
[28] A. K. Ziarani and A. Konrad, "A nonlinear adaptive method of elimination of power line interference in ecg signals," *IEEE Transactions on Biomedical Engineering*, vol. 49, no. 6, pp. 540–547, 2002.
[29] S. M. Martens, M. Mischi, S. G. Oei, and J. W. Bergmans, "An improved adaptive power line interference canceller for electrocardiography," *IEEE Transactions on Biomedical Engineering*, vol. 53, no. 11, pp. 2220–2231, 2006.
[30] O. T. Inan and G. T. Kovacs, "An $11mu$ w, two-electrode transimpedance biosignal amplifier with active current feedback stabilization," *IEEE Transactions on Biomedical Circuits and Systems*, vol. 4, no. 2, pp. 93–100, 2010.
[31] L. Fay, V. Misra, and R. Sarpeshkar, "A micropower electrocardiogram amplifier," *IEEE Transactions on Biomedical Circuits and Systems*, vol. 3, no. 5, pp. 312–320, 2009.
[32] S. Nishimura, Y. Tomita, and T. Horiuchi, "Clinical application of an active electrode using an operational amplifier," *IEEE Transactions on Biomedical Engineering*, vol. 39, no. 10, pp. 1096–1099, 1992.
[33] T. Degen and H. Jackel, "A pseudodifferential amplifier for bioelectric events with dc-offset compensation using two-wired amplifying electrodes," *IEEE Transactions on Biomedical Engineering*, vol. 53, no. 2, pp. 300–310, 2006.
[34] R. Pallas-Areny, J. Colominas, and J. Rosell, "An improved buffer for bioelectric signals," *IEEE Transactions on Biomedical Engineering*, vol. 36, no. 4, pp. 490–493, 1989.